ChemistrySelect

Research Article
doi.org/10.1002/slct.202405466

Chemistry Europe
European Chemical Societies Publishing

www.chemistryselect.org

Enhanced Drug Delivery of Platinum(II) Complexes Using Acetamide-Functionalized PAMAM Dendrimers: Synthesis, Characterization, and Anticancer Activity Against A549 Lung Cancer Cells

Nthabiseng Manama,[a] Tebogo Peega,[a] Leonie Harmse,[b] and Izak A. Kotzé*[a]

Since the discovery of cisplatin, extensive research has been conducted on platinum-based complexes aimed at reducing toxicity and improving selectivity. Drug delivery systems such as poly(amidoamine) (PAMAM) dendrimers have emerged as promising carriers due to their biocompatibility, tunable surface chemistry, and potential to overcome issues such as low solubility and poor selectivity. In this study, Generation 4 (G4) and Generation 5 (G5) PAMAM dendrimers, along with acetamide-functionalized counterparts (Gn-Ac), were synthesized and characterized. Additionally, a series of platinum(II) complexes incorporating *N,N*-di(alkyl)-*N'*-acylthiourea and 1,10-phenanthroline (phen) derivatives (PtL1, PtL2, and PtL3) were prepared. Host–guest interactions between the dendrimers and the platinum complexes were studied using ^{1}H NMR, DOSY NMR, and viscosity measurements, revealing notable chemical shift changes, significant decreases in diffusion coefficients, and increases in viscosity upon encapsulation. Cytotoxicity screening against the A549 lung cancer cell line showed that dendrimer-platinum aggregates involving acetamide-functionalized dendrimers exhibited reduced toxicity compared to non-functionalized dendrimers. Furthermore, dendrimer cavity size influenced interaction strength, with the G5-Ac dendrimer displaying stronger interactions with PtL3, as confirmed by NOE cross-peaks between the complex protons and the internal dendrimer protons. Lastly, the known anticancer agent 5-fluorouracil (5-FU) was successfully encapsulated in G5 dendrimers and used as a positive control in anticancer in vitro screening.

1. Introduction

Platinum-based complexes have demonstrated significant anticancer activity, particularly since the serendipitous discovery of cisplatin. However, cisplatin exhibits considerable toxicity due to its lack of selectivity, impacting both cancerous and healthy cells. Recent research has shifted toward the development of platinum(II) complexes that are less toxic, particularly by incorporating ligands with their own anticancer properties.[1–5] Among these, complexes containing 1,10-phenanthroline and acylthiourea ligands have attracted considerable attention. Phenanthroline, due to its intercalative ability, and thiourea-based ligands present a promising combination. The [Pt(phen)(*N,N*-di(alkyl)-*N'*-acylthiourea)]Cl complexes, as shown by Peega et al., have shown antiproliferative activity that outperforms cisplatin with IC_{50} values of 0.68–2.28 μM compared to 12.5–19.4 μM for 3 cancer cell lines.[6] However, some of these complexes face challenges related to insufficient solubility and selectivity, limiting their clinical potential.

To address these issues, the use of dendrimers as drug delivery systems (DDSs) has been proposed. Dendrimers are nanoscale, hyperbranched polymeric structures, known for their controlled, uniform size, monodispersity, and versatile surface functionalization. Structurally, dendrimers consist of a central core, internal branching units (dendrons), and surface functional groups. These surface groups can be modified to conjugate with biomolecules, such as antibodies or drugs, making them particularly useful for targeted drug delivery. Additionally, the internal cavities within dendrimers allow for the encapsulation of therapeutic molecules, forming stable host–guest complexes.

Polyamidoamine (PAMAM) dendrimers, first synthesized by Tomalia et al., are among the most widely studied dendritic polymers for drug delivery applications due to their monodisperse structure, internal voids, and modifiable surface chemistry.[7] These dendrimers consist of a central ethylenediamine core and repeating units of methyl acrylate and ethylenediamine, forming generations characterized by exponential growth in terminal groups. The regularity and controllability of their architecture allow for precise tuning of both physicochemical properties and drug loading capacity.

[a] *N. Manama, T. Peega, I. A. Kotzé*
Molecular Sciences Institute, School of Chemistry, University of the Witwatersrand, Private Bag X3, Wits, Johannesburg 2050, South Africa
E-mail: Izak.Kotze@wits.ac.za

[b] *L. Harmse*
Division of Pharmacology, Department of Pharmacy and Pharmacology, Faculty of Health Sciences, University of the Witwatersrand, Johannesburg, South Africa

Supporting information for this article is available on the WWW under https://doi.org/10.1002/slct.202405466

Despite these advantages, PAMAM dendrimers, particularly those terminated with primary amines, are known to exhibit significant cytotoxicity due to their cationic surface charge. This charge can lead to undesirable interactions with cellular membranes, causing membrane disruption and oxidative stress. A recent review by Singh et al. (2024) has compared the biological performance of different dendrimer types and concluded that surface modification strategies are essential for improving both safety and pharmacokinetics of PAMAM-based carriers.[8] Among these modifications, acetylation of terminal amine groups has proven particularly effective in neutralizing surface charge without compromising the dendrimer's ability to encapsulate or conjugate with drugs. Acetylated PAMAM dendrimers demonstrate lower cytotoxicity, enhanced biocompatibility, and greater stability in physiological environments. The Singh et al. review further highlights the suitability of Generation 4 (G4) and Generation 5 (G5) PAMAM dendrimers for drug delivery, noting a favorable balance between size, loading capacity, and reduced toxicity profiles.[8]

To explore this potential, we synthesized and characterized various [Pt(phen)(*N,N*-di(alkyl)-*N*''-acylthiourea)]Cl complexes and encapsulated them using acetylated G4 and G5 PAMAM dendrimers. The resulting host–guest complexes were analyzed using various NMR techniques. Additionally, 5-fluorouracil (5-FU) was encapsulated within acetylated PAMAM dendrimers as a reference compound. Both the host–guest complexes and the free [Pt(phen)(*N,N*-di(alkyl)-*N*''-acylthiourea)]Cl complexes were evaluated for their anticancer activity through screening against the lung cancer cell line A549. This study aims to assess the potential of dendrimer-based delivery systems to enhance the solubility, stability, and efficacy of platinum-based anticancer agents.

2. Results and Discussion

2.1. Synthesis and Characterization of [Pt(phen)(L^n-O,S)]$^+$ Complexes

The synthesis of the Pt(II) complexes involved preparing the *N,N*-di(alkyl)-*N*''-acylthiourea ligand and the $PtCl_2$(phen) precursor. These were then reacted in a 1:1 ratio in the presence of sodium acetate (NaOAc), which facilitated ligand deprotonation, favoring the formation of the desired bidentate complex, as shown in Figure 1. Adding 4% water to the reaction mixture minimized unwanted side products, such as the formation of bis-monodentate acylthiourea complexes.[9] The *N,N*-di(butyl)-*N*''-benzoylthiourea ligand was synthesized using the method described by Douglas and Dains[10] (detailed in the Experimental Section) and was isolated as colorless crystals with a yield of 78%.

The $PtCl_2$(phen) precursor was synthesized according to the method of Morgan and Burstall[11] (described in the experimental section) and was isolated as a bright yellow powder with a yield of 88%. The resulting [Pt(phen)(L^n-*O,S*)]$^+$ complexes were obtained as yellow–brown powders, with yields ranging from 66% to 75%. These were characterized using 1D and 2D NMR spectroscopy, IR spectroscopy, mass spectrometry, and elemental analysis where applicable.

The ^{1}H NMR spectrum of [Pt(phen)(*N*'-pivaloyl-*N,N*-diethylthiourea)]$^+$ (PtL_3) in $CDCl_3$ is shown in Figure 2.

Upon complexation, the precursor loses its symmetry, as indicated by the peaks assigned to protons 1–8. The absence of the N—H signal, previously observed downfield in the free ligand, further confirms the bidentate coordination of the complex. The aliphatic region was assigned using 2D NMR spectroscopy. The sharp singlet at 1.35 ppm, integrating for nine protons, corresponds to the chemically equivalent CH_3 groups of the pivaloyl moiety. Proton pairs H^a and $H^{a'}$ and H^b and $H^{b'}$ are not chemically equivalent due to the partial double bond character of the thio-amidic bond. Additionally, the broad singlet at 2.50 ppm is attributed to residual water, while the singlet at 2.08 ppm is due to acetic acid, a side product formed during the ligand's deprotonation by NaOAc.

The ^{1}H NMR spectral changes provide strong evidence of successful complexation. Variations in the *N,N*-di(alkyl)-*N*'-acylthiourea ligand were introduced to study the effect of the ligand on the host–guest interactions between the complexes and dendrimers. The synthesized complexes are labeled with their respective abbreviations, as shown in Figure 1.

2.2. Synthesis and Characterization of PAMAM Dendrimers and Acetamide-Functionalized PAMAM (Gn-Ac)

The divergent synthesis approach described by Tomalia et al. was used to produce Generation 4 (G4) PAMAM dendrimers.[7] Generations 1.5 and higher were purified by dialysis against methanol using cellulose membranes (1.5, 6, and 14 kDa depending on the molecular mass of each half-generation). The detailed synthesis and characterization of the half-generation (Gn0.5) up to full-generation (Gn) PAMAM dendrimers and intermediates are described in the Supporting Information.

Amine-terminated PAMAM dendrimers are known to become protonated at physiological pH in vivo, resulting in the formation of positively charged species (R-NH_3^+), which exhibit greater toxicity compared to their neutral or anionic counterparts due to their propensity to induce cell lysis.[12,13] To mitigate this issue, the NH_2 groups were converted to non-ionizable acetamide groups ($NHCOCH_3$), which are expected to improve the pharmacological profile of the dendrimer. The neutralization of the dendrimer periphery is expected to enhance the encapsulation efficiency of our cationic platinum(II) complexes.

Acetamide-functionalized G4 and G5 PAMAM dendrimers were synthesized using the method described by Li et al.[14] In this process, acetic anhydride (Ac_2O) and triethylamine (TEA) were added to a methanolic solution of amine-terminated dendrimer (Gn-NH_2) under an inert atmosphere, allowing the reaction to proceed for 24–48 h, depending on the dendrimer generation. The G4-Ac dendrimer was used as a model for characterization of acetamide-functionalized PAMAM (Figure 3).

The appearance of a singlet at 1.6 ppm, integrating for 192 protons, corresponds to the methyl groups of the

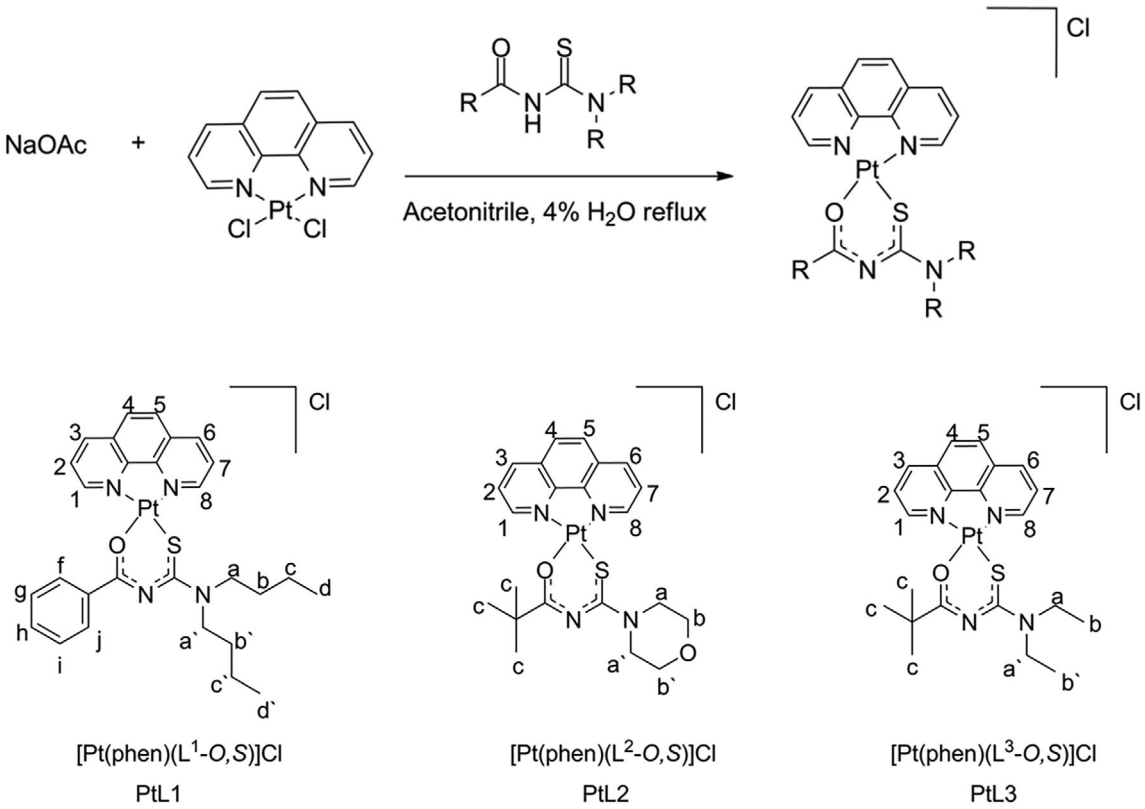

Figure 1. General synthesis of [Pt(phen)(*N,N*-di(alkyl)-*N'*-acylthiourea)]Cl complexes with chemical structures of synthesized [Pt(phen)(L^n-O,S)]Cl complexes and their abbreviations.

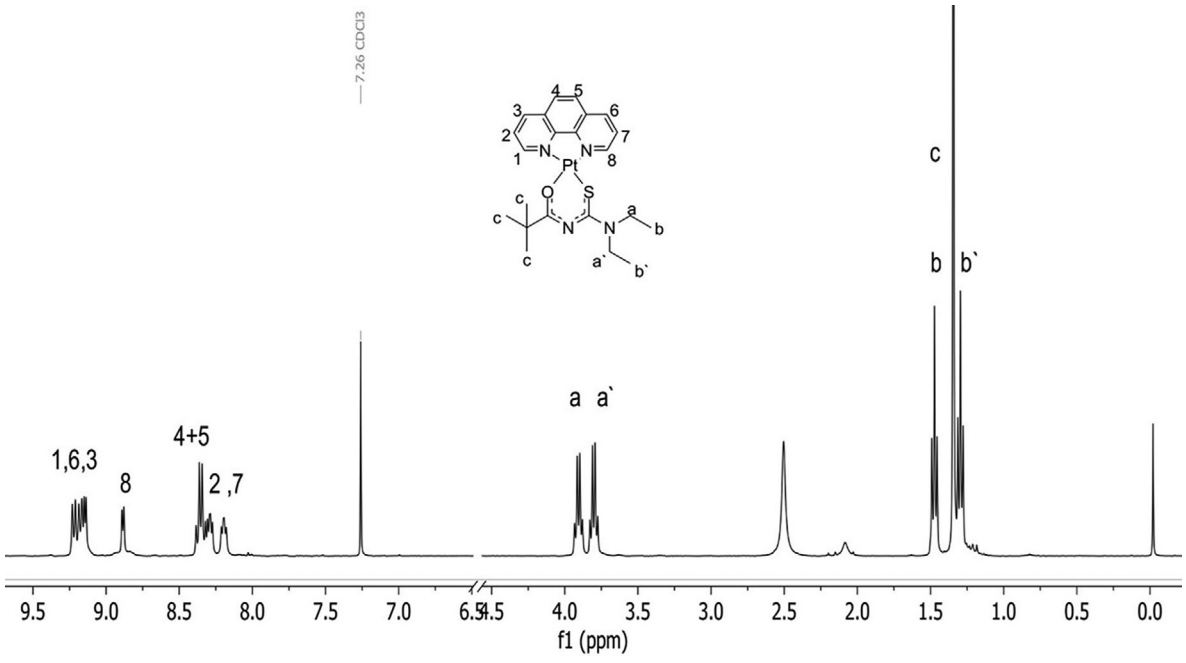

Figure 2. ^{1}H NMR of [Pt(phen)(*N'*-pivaloyl-*N,N*-diethylthiourea)]$^+$ (PtL3) in $CDCl_3$ at 300 K.

acetamide moieties, confirming the successful conversion of all amine groups (NH_2) to acetamide ($NHCOCH_3$). The remaining peaks were assigned, with $H^{g'}$ shifting upfield due to the electron-withdrawing effect of the carbonyl group, further confirming the transformation. Additionally, as the dendrimer size increased, the NMR peaks broadened, reflecting the larger number of repeating units.

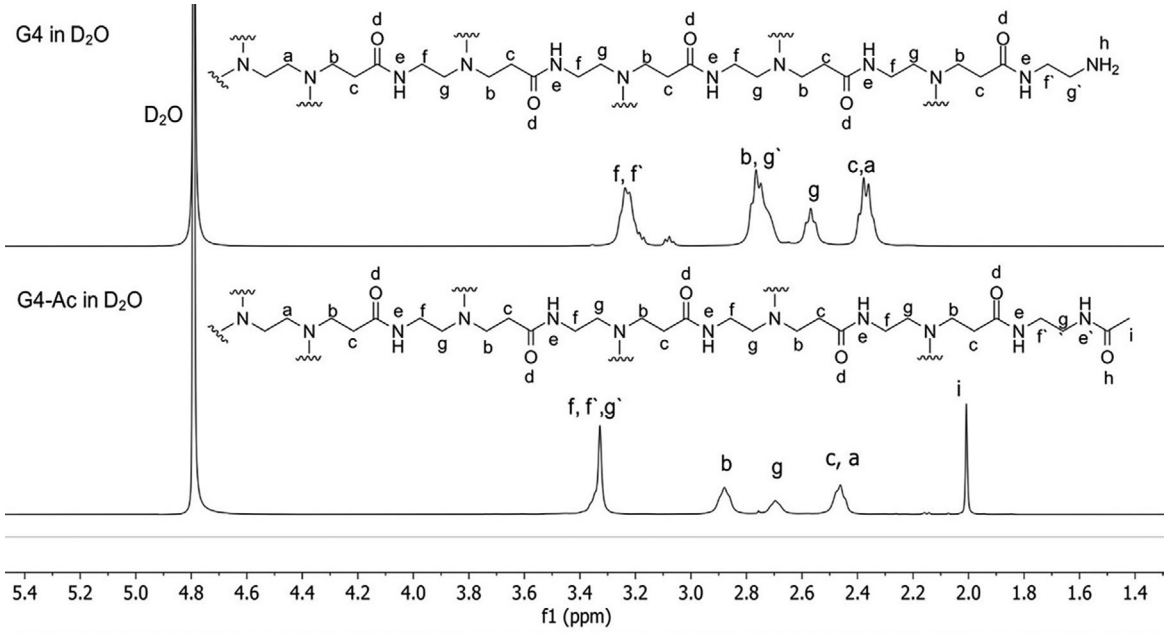

Figure 3. Stacked ^{1}H NMR spectra of amine-terminated G4 PAMAM (G4-NH_2) and acetamide-terminated G4 PAMAM (G4-Ac) in D_2O at 300 K.

The functionalized dendrimer was further characterized using MALDI-TOF mass spectrometry, which revealed an increase in molecular weight from 14.83 kDa for the amine-terminated G4 to 16.69 kDa for the acetamide-functionalized G4, as indicated by the singly charged molecular ion $[M]^+$ peaks (Figure S7). Additionally, doubly charged molecular ion peaks were observed at *m/z* 7.69 kDa for G4-Ac and m/z 7.40 kDa for the unmodified G4 dendrimer, providing further confirmation of successful acetamide functionalization.

2.3. Encapsulation of Complexes

Several encapsulation methods reported in the literature, including co-precipitation in methanol, aqueous encapsulation, biphasic dichloromethane/water approaches, and pH modulation, were explored but found ineffective. These methods failed primarily due to poor solubility, aggregation, electrostatic repulsion, or partial decomposition of the complex.[15–19]

Successful encapsulation was, however, achieved using DMSO as the solvent. The platinum complex was dissolved in DMSO-d_6 and combined with the dendrimer at a 1:15 molar ratio. The mixture was then gently stirred in the dark for 24 h, shielded by foil. NMR spectroscopy provided clear evidence of host–guest interactions, demonstrating that the hydrophobic platinum complex preferentially localizes within the dendrimer's hydrophobic cavities.

We are confident that these complexes will occupy the dendrimer's hydrophobic cavities in a buffer solution during biological screening. Although the concentration of the adducts in the DMSO-d_6:Buffer mixture is too low for NMR spectroscopy, their behavior in DMSO-d_6 provides sufficient evidence of these interactions.

2.4. Host–Guest Interactions

The host–guest interactions between PAMAM dendrimers and platinum complexes were studied using ^{1}H NMR and DOSY NMR spectroscopy. This involved adding PtL1, dissolved in DMSO-d_6, dropwise to a solution of G4-Ac, followed by stirring in the dark. After 24 h, a ^{1}H NMR spectrum was recorded (Figure 4).

Upon mixing, changes were observed in signals from both the aliphatic and aromatic protons of the complex, indicating interactions between the dendrimer and the platinum complex. The chemical shift differences for the aliphatic protons are presented in Table S1, while the aromatic protons overlap extensively with G4-Ac NH protons for straightforward identification.

DOSY NMR experiments were conducted on both the dendrimer-complex mixture and the free complex, with constant concentrations in DMSO-d_6 to compare diffusion coefficients. Additionally, the temperature effect on the host–guest complexes was studied at 300 and 310 K. A Bayesian DOSY transformation (using the Mestrenova software suite) was applied, and the resulting spectra are shown in Figure 5.

In our case, a single set of cross-peaks corresponding to the complex are seen instead of a set of signals corresponding to the "bound" complex and another for the "free" complex (Figure 5). This indicates that the interaction between the dendrimer and complex is in fast exchange, where the complex migrates in and out of the dendrimer cavities, which suggests that it is weakly bound; this kind of interaction has been observed in large guest molecules such as surfactants.[20–22] This dynamic interaction is faster than the NMR time scale; therefore, an average between the two states is observed. The observed diffusion coefficient is therefore a molecular fraction weighted average between a "bound" and "free" guest molecule, represented by Equation (1):

$$D_{obs} = D_{bound}(\chi) + D_{free}(1 - \chi) \quad (1)$$

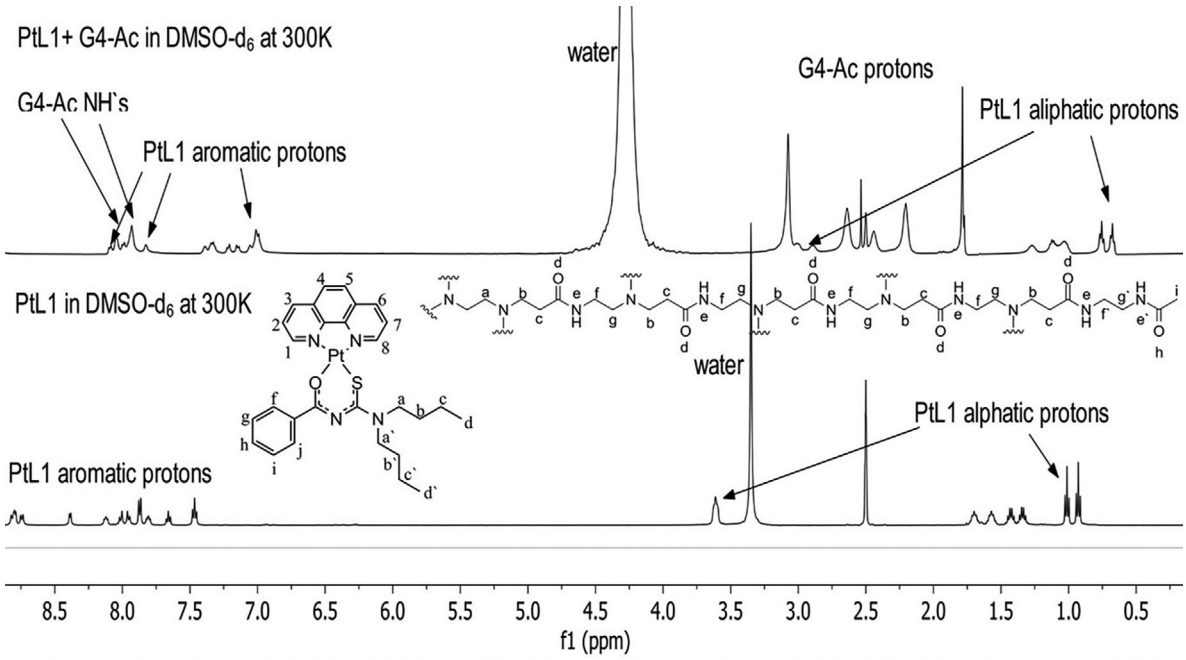

Figure 4. Stacked ^{1}H NMR spectra of PtL1 in DMSO-d_6 and G4-Ac and PtL1 encapsulation attempt in DMSO-d_6 at 300 K.

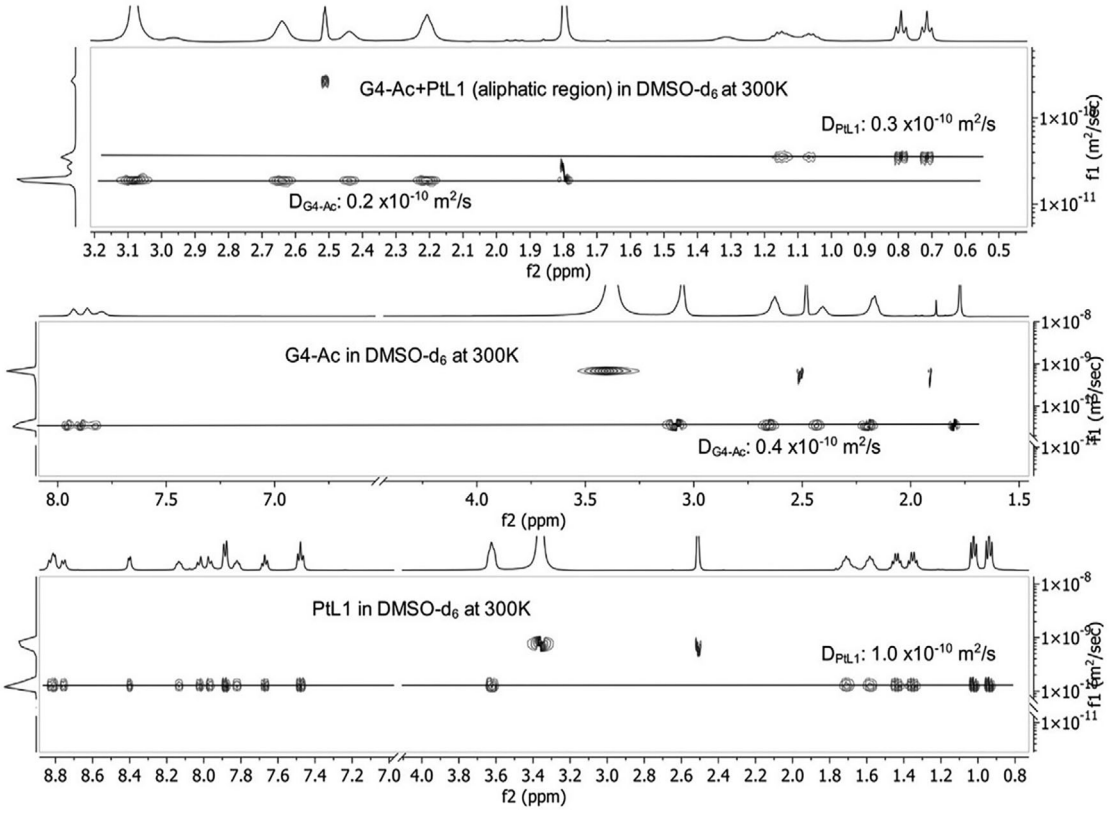

Figure 5. DOSY spectra of G4-Ac + PtL1 mixture, G4-Ac, and PtL1 in DMSO-d_6 at 300 K.

where D_{obs} is the observed diffusion coefficient, D_{bound} is the diffusion coefficient of the bound state, D_{free} represents the free state, and χ is the molecular fraction.[20]

More accurate diffusion coefficients for G4-Ac, DMSO-d_6, and PtL1 were obtained by manually fitting the data using Mestrenova software. To calculate these diffusion coefficients, integrations of specific peaks were used, applying a mono-exponential fit method. For G4-Ac, only the internal protons were considered because the surface acetamide functional groups exhibited a larger diffusion coefficient, which could introduce inaccuracies. In contrast, for PtL1, the aliphatic proton signals were used since the peak intensity is greater than the aromatic protons.

Table 1. Diffusion coefficients and hydrodynamic volume (V_H) of PtL1 + G4-Ac mixture, PtL1 in DMSO-d_6 as well as G4-Ac in DMSO-d_6 at 300 and 310 K.

	Viscosity × 10^{-3} Pa.s	Diffusion Coefficient (V_H nm^3) × 10^{-10} m^2/s		
	η	G4-Ac	PtL1	DMSO-d_6
PtL1 and G4-Ac				
300 K	4.1	0.2 (97.2)	0.3 (15.3)	2.3 (0.05)
310 K	3.0	0.4 (36.4)	0.7 (6.3)	3.2 (0.05)
PtL1				
300 K	2.5	–	1.0 (2.5)	4.8 (0.02)
310 K	2.0	–	1.4 (2.1)	6.2 (0.02)
DMSO-d_6				
300 K	2.0	–	–	6.1 (0.02)
310 K	1.7	–	–	7.7 (0.02)
G4-Ac				
300 K	2.6	0.4 (49.5)	–	4.2 (0.03)
310 K	2.1	0.5 (35.2)	–	5.4 (0.03)

To further understand the interactions between the dendrimer and the guest molecule, hydrodynamic volumes (V_H) were calculated. Viscosity measurements of the samples at 300 and 310 K were conducted using an AntonPaar Microviscometer LOVIS2000M. These viscosity values allowed for the calculation of hydrodynamic radii (R_H) using the Stokes–Einstein equation, which were then used to derive the hydrodynamic volumes (V_H). V_H is particularly useful in modeling molecular interactions, such as host–guest interactions, since it considers viscosity differences between solutions. However, a limitation of V_H is its assumption that molecules are spherical, which introduces a margin of error for nonspherical molecules. The viscosities, diffusion coefficients, and hydrodynamic volumes (V_H) at 300 and 310 K are summarized in Table 1.

The observed increase in viscosity for the mixture was not solely due to the rise in concentration but also influenced by an increase in ionic strength.[23] A similar trend was reported by Bakshi et al., who observed a rise in viscosity in dendrimer-surfactant systems upon the addition of surfactants, accompanied by dendrimer-surfactant aggregates that were concentration-dependent.[24]

To account for the observed viscosity variations, hydrodynamic volumes (V_H) were calculated. At 300 K, the V_H of DMSO remained mostly constant, except in the mixture, where an increase was noted. This suggests an interaction between the dendrimer and the solvent. Since the dendrimer cavities preferentially trap hydrophobic guest molecules, minimal DMSO was entrapped, which resulted in only a slight increase in V_H. When the platinum complex was introduced to the dendrimer, a decrease in the diffusion coefficient was observed, accompanied by an 84% increase in V_H, indicating a stronger interaction between the dendrimer and the complex than between the dendrimer and solvent. Additionally, the diffusion coefficient of the dendrimer decreased when mixed with the complex, along with a 49% increase in V_H, confirming that a host–guest interaction was occurring, as the complex-dendrimer combination diffused more slowly than G4-Ac alone.

The influence of ionic strength on dendrimer diffusion behavior was explored since the platinum complex is a salt, carrying a positive charge and a counterion. Tetrabutylammonium chloride ([TBA]Cl) was added to G4-Ac at the same concentration as the platinum complex. The ^{1}H NMR spectra, diffusion coefficients, and viscosity measurements were recorded, and the respective hydrodynamic volumes (V_H) were calculated, as summarized in Table 2. No significant changes in the chemical shift or peak shape of [TBA]Cl were observed upon its addition to the dendrimer, as shown in Figure S8, in contrast to the noticeable shifts seen with the PtL1 complex (Figure 4). However, an increase in viscosity was once again detected in the mixture, attributable to the rise in ionic strength. At 300 K, the V_H of plain DMSO was calculated to be 0.02 nm^3, whereas the V_H of G4-Ac, TBA[Cl], and the G4-Ac-[TBA]Cl mixture was measured at 0.03 nm^3 (Table 2).

This increase in V_H indicates interactions between DMSO, G4-Ac, and [TBA]Cl. Interestingly, while [TBA]Cl exhibited a 40% decrease in V_H, G4-Ac showed a 31% increase, alongside a reduction in the diffusion rates of both species in solution. This suggests dendrimer aggregation rather than [TBA]Cl encapsulation, a phenomenon previously reported in polymeric systems under increased ionic strength.[23,25] These findings further support the formation of a host–guest complex between the platinum complex and the dendrimer, as evidenced by the increase in V_H upon the introduction of the platinum complex to the dendrimer.

At 310 K, a general decrease in V_H was observed across all samples, with the most significant reduction occurring in G4-Ac within the mixture, where a 69% decrease was recorded. This suggests that the dendrimer aggregates are disrupted at higher temperatures.

To compare these findings with different dendrimer sizes, G5-Ac was tested against G4-Ac. An excess of PtL3 in a DMSO-d_6/D_2O (6:1) mixture was added to G5-Ac, and an excess of PtL2 was added to G4-Ac. The D_2O was used to aid in the dissolution of the dendrimers. Both mixtures were stirred in the dark for 24 h, and the resulting ^{1}H NMR and NOESY spectra were recorded (Figure 6).

In the G5-Ac and PtL3 mixture (left), broadening of the aromatic proton signals was observed, likely due to the combined effects of water (D_2O) and interactions with the dendrimer. NOE cross-peaks were observed between the aromatic protons of the complex and the internal protons of the dendrimer, indicating a measurable interaction with G5-Ac compared to G4-Ac, likely due to the larger cavities in G5-Ac. Similar results were obtained by Fang et al., who reported NOEs between guest molecules and both G5 and G5-Ac, but none for G4 or G4-Ac.[26]

2.5. In Vitro Anticancer Cytotoxicity Screening of PAMAM-Encapsulated Complexes

The anticancer activity of PAMAM-encapsulated platinum complexes was evaluated against the lung cancer cell line A549, with 5-fluorouracil (5-FU) as a control. Platinum complexes PtL1

Table 2. Viscosity, diffusion coefficients, and hydrodynamic volume (V_H) of [TBA]Cl + G4-Ac mixture, [TBA]Cl as well as G4-Ac in DMSO-d_6 at 300 and 310 K.

	Viscosity × 10^{-3} Pa.s	Diffusion Coefficient (V_H nm^3) × 10^{-10} m^2/s		
	η	G4-Ac	[TBA]Cl	DMSO-d_6
[TBA]Cl and G4-Ac				
300 K	3.2	0.3 (71.5)	1.7 (0.3)	3.5 (0.03)
310 K	2.5	0.5 (22.4)	2.4 (0.2)	5.1 (0.02)
[TBA]Cl				
300 K	1.9	–	2.4 (0.5)	6.1 (0.03)
310 K	1.6	–	3.2 (0.4)	7.8 (0.03)
DMSO-d_6				
300 K	2.0	–	–	6.1 (0.02)
310 K	1.7	–	–	7.7 (0.02)
G4-Ac				
300 K	2.6	0.4 (49.5)	–	4.2 (0.03)
310 K	2.1	0.5 (35.2)	–	5.4 (0.03)

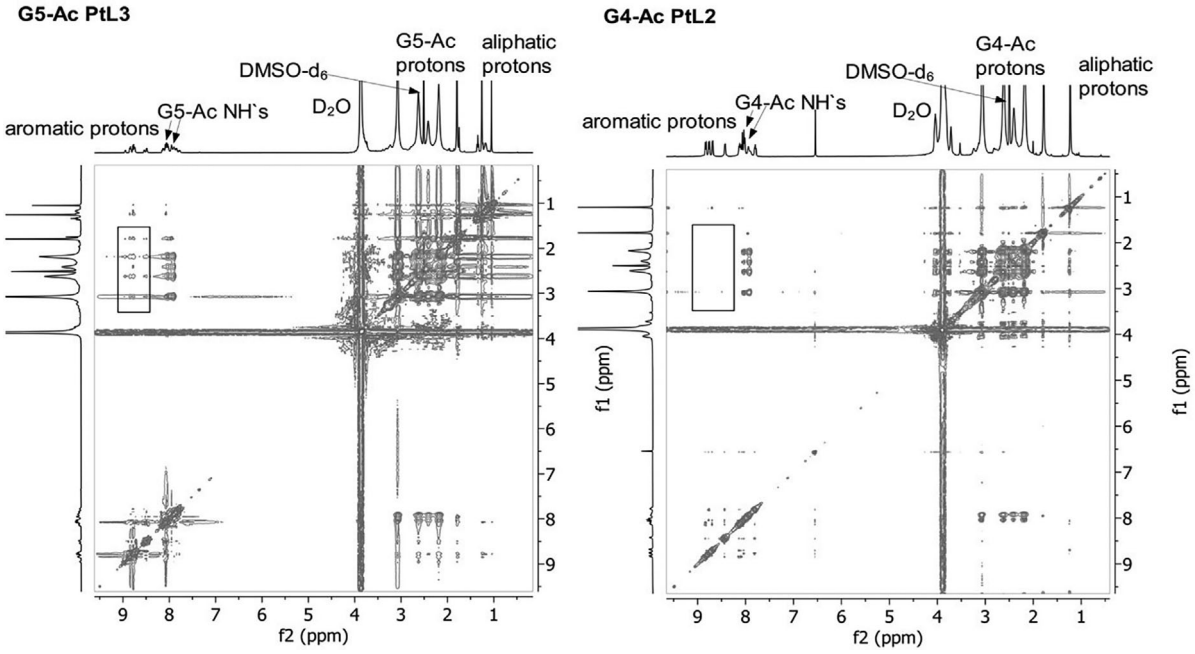

Figure 6. NOESY spectrum of PtL3 and G5-Ac mixture (left) and PtL2 and G4-Ac mixture (right) in DMSO-d_6 and D_2O (6:1) at 300 K.

and PtL2 were encapsulated using acetamide-functionalized G4 PAMAM dendrimers (G4-Ac), while PtL3 was encapsulated with G5-Ac. Additionally, 5-FU was encapsulated within the G5 dendrimer following a procedure previously reported for successful encapsulation of 5-FU with G3 PAMAM dendrimers.[27,28]

At 50 μM, free platinum complexes (PtL1, PtL2, and PtL3) were highly cytotoxic, leading to near-complete inhibition of cell growth, with cell viabilities of 0.4% ± 0.3%, 0.9% ± 0.3%, and 0.0% ± 0.0%, respectively (Figure 7a). Similarly, their corresponding dendrimer-encapsulated complexes showed comparable cytotoxicity, with G4-Ac + PtL1, G4-Ac + PtL2, and G5-Ac + PtL3 exhibiting cell viabilities of 0.0% ± 0.0%, 0.8% ± 0.5%, and 0.0% ± 0.0%, respectively (Figure 7a).

At 5 μM, the platinum complexes maintained potent cytotoxicity, with cell viabilities below 40% (Figure 7b). PtL1 demonstrated the most potent cytotoxic effect, with only 8.2% ± 1.2% viable cells, while PtL2 and PtL3 were less effective, with cell viabilities of 39.0% ± 2.0% and 30.2% ± 1.9%, respectively. Encapsulation with functionalized dendrimers enhanced the activity of PtL1 and PtL2, reducing cell viability to 6.9% ± 1.2% and 33.9% ± 1.7%, respectively, representing improvements of 1.3% and 3.7%. Conversely, PtL3 encapsulation slightly reduced its activity, with cell viability increasing to 35.6% ± 1.9% (a 5.4% reduction in activity).

In contrast, 5-FU was poorly cytotoxic compared to the platinum complexes, with cell viabilities above 55% at both concentrations. At 50 μM, 5-FU resulted in 62.3% ± 4.1% cell viability,

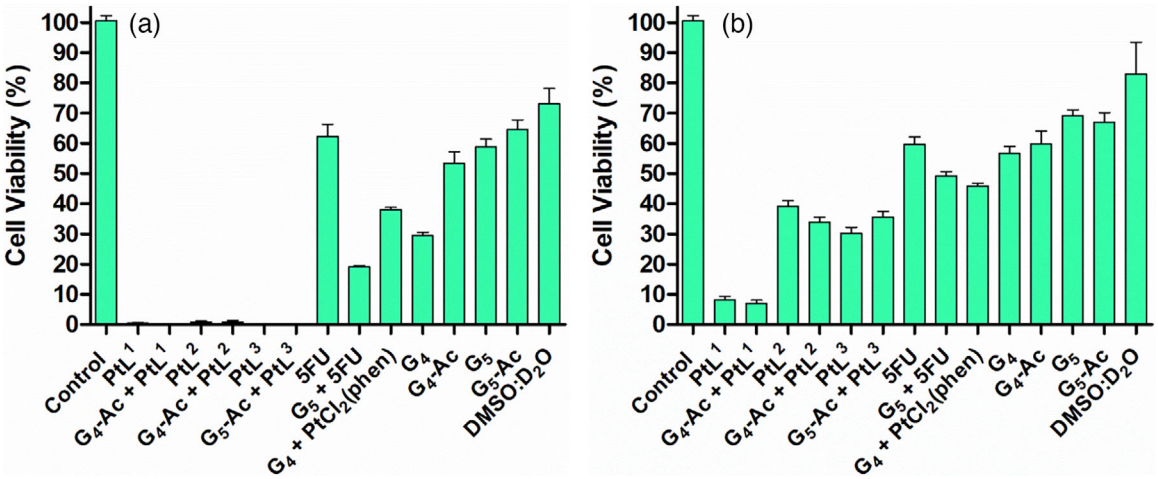

Figure 7. Cell viability in A549 cells after a 48-h treatment with free and dendrimer-encapsulated platinum complexes, dendrimers, and 5-FU, at concentrations of a) 50 μM and b) 5 μM.

while at 5 μM, cell viability was 59.6% ± 2.4%. Encapsulation of 5-FU in G5 significantly enhanced its activity, reducing cell viability to 19.1% ± 0.4% at 50 μM (a 43.1% improvement) and to 49.2% ± 1.3% at 5 μM (a 10.5% improvement).

The free dendrimers G4 and G5 displayed limited yet significant cytotoxicity. At 50 μM, free G4 and G5 resulted in cell viabilities of 29.4% ± 1.2% and 58.8% ± 2.6%, respectively, while at 5 μM, the cell viabilities were 56.6% ± 2.4% and 69.1% ± 2.0%, respectively. Acetamide-functionalized dendrimers (G4-Ac and G5-Ac) further reduced cytotoxicity compared to their unmodified counterparts. At 50 μM, G4-Ac and G5-Ac exhibited cell viabilities of 53.3% ± 4.0% and 64.5% ± 3.3%, respectively, while at 5 μM, they showed viabilities of 59.8% ± 4.2% and 67.0% ± 3.2%, respectively. These results indicate low cytotoxicity effects of the dendrimers, with G5 showing lower intrinsic cytotoxicity.

The solvent mixture DMSO:D_2O (6:1), used in the preparation of the complexes, was also tested for its cytotoxicity. The solvent exhibited minimal cytotoxicity compared to the complexes, with cell viabilities of 73.1% ± 5.0% at 50 μM and 82.9% ± 10.5% at 5 μM. Thus, the observed cytotoxicity in the treated samples can be primarily attributed to the platinum complexes and the dendrimers.

3. Conclusions

In this study, we synthesized and characterized Generation 4 (G4) and Generation 5 (G5) PAMAM dendrimers, along with their acetylated counterparts (Gn-Ac), and prepared various mixed ligand cationic platinum (II) complexes of *N,N*-di(alkyl)-*N'*-acylthiourea and 1,10-phenanthroline derivatives. Using ^{1}H NMR, DOSY NMR, and viscosity measurements, we investigated the host–guest interactions between these platinum complexes and the dendrimers. The results showed that the dendrimers encapsulated the platinum complexes, leading to significant changes in chemical shifts, diffusion coefficients, and viscosity. These shifts suggest the formation of aggregates with dynamic interactions with the dendrimer cavities in DMSO-d_6.

In vitro, the cytotoxicity of the free platinum complexes and their dendrimer-encapsulated counterparts was evaluated against the A549 lung cancer cell line. At higher concentrations, both free and dendrimer-encapsulated platinum complexes demonstrated potent cytotoxic effects, with cell viability approaching zero. Even at lower concentrations, the complexes retained substantial cytotoxicity, with the dendrimer-encapsulated versions generally showing improved or comparable activity.

The results confirmed that PAMAM dendrimers, particularly the acetylated versions, have strong potential as drug delivery vehicles. They not only reduce the inherent toxicity of the dendrimers but also enhance the efficacy of platinum complexes. Furthermore, larger dendrimers like G5 showed more evidence of stronger interactions with the platinum complexes, suggesting that the size of the dendrimer influences the encapsulation process and the resulting anticancer activity.

In conclusion, this study demonstrates that dendrimer-based drug delivery systems could be a promising approach to enhancing the potential of platinum-based anticancer drugs. With future periphery modification, dendrimers can provide a platform that can be further developed to increase the therapeutic index of these potent anticancer agents by enhancing solubility, reducing toxicity, and introducing selectivity.

4. Experimental Section

Instrumentation and reagents: All reagents were purchased from Sigma-Aldrich and used without further purification. L2 and L3 were used as prepared previously.[29] Acetone and methanol were dried using the appropriate drying agents as described in literature and distilled prior to use.

NMR experiments were recorded on a Bruker Avance 300 MHz and Bruker Avance 400 MHz spectrometer. Spectra were recorded in deuterated solvents (chloroform-d_1, D_2O, methanol-d_4, and DMSO-d_6). Chemical shifts are reported relative to each respective solvent

and are reported in parts per million (ppm) and coupling constants are reported in Hertz (Hz). ESI mass spectrometry was recorded on a Bruker Compact Ultimate 300 HR-MS spectrometer. MALDI-TOF mass spectrometry was recorded on a Bruker Autoflex TOF/TOF spectrometer in a 2,5-dihydroxybenzoic acid (DHB) and sodium triflate matrix. FT-IR experiments were recorded on a Bruker TENSOR 27 spectrometer using both KBr and ATR.

4.1. Synthesis of $PtCl_2$(phen) Precursor

The precursor was synthesized according to the method described by Morgan and Burstall.[11] Potassium tetrachloroplatinate (204.0 mg, 0.49 mmol) was added to a round-bottom flask with 30 mL deionized water and 4 drops of 32% HCl. The mixture was stirred for 10 min. 1.10-phenanthroline (89 mg, 0.49 mmol) was then added to the reaction vessel and the mixture was refluxed for 3 h. The yellow product was washed with water (to remove unreacted potassium tetrachloroplatinate), followed by acetonitrile (to remove unreacted and lastly, diethyl ether. The product was then dried under vacuum. The results obtained are reported below:

$PtCl_2$(phen), Yield: 80.4%. ^{1}H NMR (300 MHz, DMSO-d_6, 300 K) δ(ppm)= 9.71 (dd,2H, ^1J: 6 Hz, ^2J: 3 Hz, **1, 8**), 9.05 (dd, 2H, ^1J: 6 Hz, ^2J: 3 Hz **3, 6**), 8.30 (s, 2H, **4, 5**), 8.20 (dd, 2H, ^1J: 6 Hz, ^2J: 3 Hz **2, 7**). FT-IR v(cm^{-1}): 3058.24 (=C—H aromatic), 1627 (C=N aromatic), 1578.20 (C=C aromatic). HRMS (ESI-MS, Calc, found, *m/z*) $[M+H]^+$ (446.974, 446.9518).

4.2. Synthesis of *N,N*-Di(butyl)-*N′*-benzoylthiourea Ligand

The *N,N*-di(butyl)-*N′*-benzoylthiourea ligand was synthesized according to a method described by Douglas and Dains.[10] Potassium thiocyanate was dried in an oven for 1 h at 150 °C followed by drying under vacuum for 1 h. Benzoyl thiourea (2.3 mL, 19. 80 mmol) was dissolved in 20 mL of anhydrous acetone and added to (2.00 g, 20 mmol) potassium thiocyanate dissolved in 25 mL anhydrous acetone and heated to reflux for 1 h. After cooling to room temperature, dibutylamine (3.8 mL, 22.55 mmol) was dissolved in 10 mL anhydrous acetone was added dropwise to the reaction vessel. The reaction was then heated to reflux for 2 h. The reaction vessel was then left to cool and allow a solid to precipitate. The solid was filtered. The remaining solution was washed with cold isopropanol and water in a 2:3 ratio. The product (colorless crystals) was recrystallized in isopropanol and left to dry under vacuum.

***N,N*-Di(butyl)-*N′*-benzoylthiourea**: Yield: 78%.%, ^{1}H NMR (300 MHz, $CDCl_3$, 300 K) δ(ppm)= 8.39 (s, 1H, **e**), 7.82 (d, 2H, 9 Hz, **f, j**), 7.57(t, 1H, 6 Hz, **h**), 7.43 (t, 2H, 9 Hz, **g, i**), 3.97 (t, 2H, 6 Hz, **a**), 3.54 (t, 2H, 6 Hz, **a′**), 1.79(qn, 2H, ^1J: 6 Hz, ^2J: 6 Hz, **b**), 1.65 (qn, 2H, ^1J: 6 Hz, ^2J: 6 Hz, **b′**), 1.45 (st, 2H, ^1J: 9 Hz, ^2J: 6 Hz, **c**), 1.30 (st, 2H,^1J: 9 Hz, ^2J: 6 Hz, **c′**), 0.98 (t, 3H, 9 Hz, **d**), 0.90 (t, 3H, 9 Hz, **d′**). ^{13}C{^{1}H} NMR (400 MHz, $CDCl_3$, 300 K) δ(ppm)= 179.85 (C=O), 163.69 (C=S), 133.04 (C^h), 129.07 (C^{g+i}), 127.87 (C^{f+j}), 53.46 (C^a), 53.28 ($C^{a'}$), 30.29 ($C^{b'}$), 28.66 (C^b), 20.21 ($C^{c+c'}$), 14.01 (C^d), 13.86 ($C^{d'}$). FT-IR v(cm^{-1}): 3173 (N-H), 2956 (C—H alkane stretch), 1689 (C=O), 1532 (C=C aromatic) C=S (1371). HRMS (ESI-MS, calc, found, *m/z*) $[M+H]^+$ (293.1687, 293.1683).

4.3. Synthesis of [Pt(phen)(*N′*-acyl-*N,N*-di(alkyl)thiourea)]$^+$ Complexes

The complexes were synthesized according to a modified method described by Koch et al.[30] 50.0 mg $PtCl_2$(phen) precursor was added to a round-bottom flask in 20 mL acetonitrile and refluxed for 10 min. 1 molar equivalent of the appropriate *N,N*-di(alkyl)-*N′*-acylthiourea ligand dissolved in 15 mL acetonitrile and 1 mL distilled water was added to the reaction vessel in a dropwise manner and left to reflux for 15 min. 1.5 molar equivalent of mg sodium acetate was dissolved in 4 mL acetonitrile and 4 mL distilled water and added to the reaction vessel. The reaction mixture was left to reflux until a color change (from milky bright yellow to pale yellow) was observed. The product was worked up by removing the solvent under reduced pressure. The product was then redissolved in acetonitrile and filtered through celite (to remove insoluble salts). The solvent was removed again, and the crude product was dissolved in 5 mL dichloromethane (DCM) and transferred to a centrifuge tube containing 40 mL hexane and the product allowed to precipitate overnight in a refrigerator. The complex was then washed via centrifuge to yield a bright yellow powder, which was dried in a vacuum oven.

[Pt(phen)(*N*-benzoyl-*N,N*-dibutylthiourea]Cl: Yield 75%, ^{1}H NMR (400 MHz, $CDCl_3$, 300 K) δ(ppm)= 9.06 (d, 1H, 3 Hz, **1**), 8.98–8.91 (m, 2H, **3, 6**), 8.61 (d, 1H, 6 Hz, **8**), 8.31 (dd, 1H, ^1J: 6 Hz, ^2J: 6 Hz, **2**), 8.09–8.02 (m, 5H, **f, j, 4, 5, 7**). 7.63 (t, 1H, 9 Hz, **h**), 7.52 (t, 2H, 9 Hz, **g, i**), 3.77–3.69 (m, 4H, **a, a′**), 1.81 (qn, 2H, ^1J: 9 Hz, ^2J: 6 Hz, **b**), 1.69 (qn, 2H,^1J: 9 Hz, ^2J: 6 Hz, **b′**), 1.52 (st, 2H, ^1J: 9 Hz, ^2J: 6 Hz, **c**), 1.41 (st, 2H,^1J: 9 Hz, ^2J: 6 Hz, **c′**), 1.06 (t, 3H, 6 Hz, **d**), 0.98 (t, 3H, 6 Hz, **d′**). ^{13}C{^{1}H} NMR (400 MHz, $CDCl_3$, 300 K) δ(ppm) = 169.09 (C=O), 164.80 (C=S), 148.29 (C^8), 144.95 (C^1), 141.45 (C^6), 140.90 (C^3), 132.87 (C^h), 129.50 (C^{f+j}), 128.99 (C^{g+i}). 128.48, 128.41 (C^4, C^5), 126.78 (C^7), 127.20 (C^2), 53.73 ($C^{a'}$), 52.27 (C^a), 30.14($C^{b'}$), 29.40 (C^b), 20.49, 20.48 (C^c $C^{c'}$), 14.11 (C^d), 14.03 ($C^{d'}$). FT-IR v(cm^{-1}):2956.97 (C—H alkane stretch), 2052.97 (aromatic C—H bend), 1402.74 (C-O), 1212.91 (C-S). HRMS (ESI-MS, Calc, found, *m/z*) $[M]^+$ (666.1866, 666.1768).

[Pt(phen)(*N*-pivaloyl-*N,N*-morpholynthiourea]Cl: Yield 68%, ^{1}H NMR (400 MHz, DMSO-d_6, 300 K) δ(ppm) = 9.05 (d, 1H, *J* = 8 Hz, **1**), 8.97 (d, 1H, *J*: 8 Hz, **6**), 8.89 (d, 1H, *J*: 8 Hz, **3**), 8.69 (d, 1H,*J*: 8 Hz **2**), 8.32–8.22 (m, 3H, **4, 5, 2**), 7.96 (dd, 1H, J_1: 8 Hz, J_2: 8 Hz, **7**), 4.12 (dd, 4H, *J*: 4 Hz, **a, a′**), 3.86 (t, 2H, *J*: 4 Hz, **b**), 3.76 (t, 2H, *J*: 4 Hz, **b′**), 1.30 (s, 9H, **c**). ^{13}C{^{1}H} NMR (400 MHz, DMSO-d_6, 300 K) δ(ppm) = 184.43 (C=O), 164.62 (C=S), 149.75 (C^8) 144.89 (C^3), 140.88 (C^6), 140.37 (C^1), 128.08, 128.02 (C^4, C^5), 126.64 (C^2), 126.30 (C^7), 66.72 ($C^{b'}$), 66.49 (C^b), 49.90 (C^a), 47.30 ($C^{a'}$), 41.52 (C^{tBu}), 28.59 (C^c). FT-IR v(cm^{-1}): 2967.91 (C—H alkane stretch), 2054.95 (aromatic C—H bend), 1431.57 (C—O), 1229.78 (C—S). HRMS (ESI-MS, calc, found, *m/z*) $[M]^+$ (604.1346, 604.1288).

[Pt(phen)(*N*-pivaloyl-*N,N*-diethylthiourea]Cl: Yield 66%, ^{1}H NMR (400 MHz, $CDCl_3$, 300 K) δ(ppm)= 9.24–9.19 (3H, **1, 3, 6**), 8.95 (d, 1H, 4 Hz, **8**), 8.43–8.38 (m, 2H, **4, 5**), 8.29 (dd, 1H, J_1: 8 Hz, J_2: 4 Hz, **2**), 8.22 (dd, 1H, J_1: 8 Hz, J_2: 4 Hz, **7**). 3.92 (q, 2H, 8 Hz, **a**), 3.81 (q, 2H, 8 Hz, **a′**), 1.49 (t, 3H, 8 Hz, **b**), 1.36 (s, 9H, **c**), 1.30 (t, 3H, 8 Hz, **b**). ^{13}C{^{1}H} NMR (400 MHz, $CDCl_3$, 300 K) δ(ppm) = 184.36 (C=O), 164.72 (C=S), 148.84 (C^8), 144.70 (C^1), 141.62 (C^6), 141.11 (C^3), 128.78 (C^4), 128.71 (C^5), 126.64 (C^7), 126.42 (C^2), 47.99 (C^a), 46.43 ($C^{a'}$), 41.79 (C^{tBu}), 28.96 (C^c), 13.11 ($C^{b'}$), 12.48 (C^b). FT-IR v(cm^{-1}): 2972.95 (C—H alkane stretch), 2051.97 (aromatic C—H bend), 1432.05 (C—O), 1251.92 (C—S). HRMS (ESI-MS, Calc, found, *m/z*) $[M]^+$ (590.1553, 590.1462).

4.4. General Acetamide-Functionalization of PAMAM Dendrimer (G_n-Ac)

The acetamide-functionalization was conducted using the method described by Li et al.[14] The amine terminated PAMAM dendrimer was dissolved in anhydrous methanol followed by the addition of a 600 molar excess of triethylamine (TEA) to the reaction vessel while stirring. A 30 molar excess of acetic anhydride was then added to the reaction mixture while kept under inert atmosphere. The

reaction was kept stirring in the dark for 24 h for G4 PAMAM and 48 h for G5 PAMAM. The product was purified by dialysis (MWCO 6 kDa) against distilled water. The water was then removed to obtain the acetylated PAMAM, which was isolated as a colorless viscous oil.

G4-Ac: Yield: 94%. ^{1}H NMR (400 MHz, D_2O, 300 K) δ(ppm) = 3.30–3.28 (m, 376H, **f, f', g'**), 2.86–2.81 (m, 248H, **b**), 2.67–2.63 (m, 120H, **g**), 2.44–2.39 (m, 252H, **c, a**), 1.96 (s, 192H, **i**). ^{13}C{^{1}H} NMR (400 MHz, D_2O, 300 K), δ (ppm) = 174.76 (**d**), 174.10 (**h**), 51.31 (**g**), 48.08 (**b, a**), 38.68, 38.66 (**f', g'**), 36.55 (**f**), 31.49 (**c**), 21.72 (**i**). FT-IR v(cm^{-1}): 3357 (N-H stretch), 2953 (C-H stretch), 1631 (C═O). Mass spectrometry (MALDI-TOF) $[M]^+$ found: 16.69 kDa.

G5-Ac: Yield 83%.^{1}H NMR (400 MHz, D_2O, 300 K) δ(ppm) = 3.25–2.23 (m,761H, **f, f' g'**), 2.76–2.72 (m, 504H, **b**), 2.57–2.54 (m, 248H, **g**), 2.36–2.32 (m, 509H, **a, c**), 1.91(s, 304H, **i**). ^{13}C{^{1}H} NMR (400 MHz, D_2O, 300 K), δ (ppm) = 174.85 (**d**), 174.00 (**h**), 51.19 (**g**),48.98 (**b, a**), 38.65, 38.57 (**f' g'**), 36.71 (**f**), 32.61 (**c**), 21.92 (**i**). FT-IR v(cm-1): 3352 (N-H stretch), 1635 (C═O). Mass spectrometry (MALDI-TOF) $[M]^+$ found: 33.18 kDa.

4.5. Cell Culture

A549 lung cancer cells were purchased from the Fox Chase Cancer Center (USA) and authenticated using short tandem repeat analysis (Inqaba Biotechnical Industries, South Africa). Cells were grown in sterile conditions in 75 cm^2 cell culture flasks (Greiner Bio-One, Separations, South Africa) at 37 °C in a 5% CO_2, humidified incubator. The cells were maintained in a 50/50 (v/v) mixture of Dulbecco's Modified Eagle Medium (DMEM) and Ham's F-12 medium (Sigma-Aldrich/Merck, SA) supplemented with 1% (v/v) sodium pyruvate and 1% (v/v) L-glutamine. Complete media contained 10% (v/v) heat-inactivated fetal bovine serum (Gibco, Thermo Fisher, Life Technologies, SA). Cells were routinely checked for mycoplasma contamination using fluorescence microscopy and Hoechst 33,342. When cells reached approximately 80% confluency, they were sub-cultured by trypsinization.

4.6. MTT Cell Viability Assay

An MTT (3-(4,5-dimethylthiazol-2-yl)-2,5-diphenyltetrazolium bromide) assay was used to investigate the anti-proliferative activity/cytotoxicity of free and dendrimer encapsulated platinum complexes against a lung cancer cell line, A549. Cells were seeded in a 96-well plate at a density of 8×10^3 cells per well in 100 µL culture media and incubated overnight to allow adherence to the plate surface. Stock solutions of platinum complexes and 5-fluorouracil (5-FU) were prepared in DMSO:D_2O solvent mixture (6:1) for complete dissolution. These were diluted to final test concentrations (50 and 5 µM) with cell culture media. Cells were then treated with free and dendrimer-encapsulated complexes, alongside free dendrimers for 44 h. Following this, 40 µL of the MTT solution (5 mg mL^{-1}) was added to each well and cells were further incubated for 4 h. Thereafter, each 96-well plate was centrifuged at 1000 rpm for 5 min and the cell culture media and MTT solution were carefully removed from each well. Following this, 200 µL of DMSO was added to each well to dissolve the formazan crystals. Subsequently, the 96-well plate was placed on a thermoshaker and agitated at 1000 rpm for 5 min at room temperature (25 °C). The absorbance was measured using a microplate Labsystems iEMS Reader at 540 nm to measure the signal and 690 nm for background/reference. All measurements were conducted in triplicates for each concentration and the experiment was repeated at least three times.

Acknowledgments

The project was funded by the NRF Thuthuka program to (Dr Izak Kotzé) National Research Foundation (grant no: 117908). The authors are grateful to Dr Cathryn Slabber from the University of the Witwatersrand for the viscosity measurements and the NMR facility at the School of Chemistry.

Conflict of Interests

The authors declare no conflict of interest.

Data Availability Statement

The data that support the findings of this study are available in the supplementary material of this article.

Keywords: 1, 10-Phenanthroline platinum complex · 5-Fluorouracil · Drug delivery system · Lung cancer · PAMAM dendrimers

[1] B. Rosenberg, L. Van Camp, T. Krigas, *Nature* **1965**, *205*, 698–699.
[2] L. Kelland, *Nat. Rev. Cancer* **2007**, *7*, 573–584.
[3] R. Panebianco, M. Viale, V. Giglio, G. Vecchio, *Inorganics* **2024**, *12*, 167.
[4] C. M. C. Andrés, J. M. Pérez de la Lastra, E. Bustamante Munguira, C. Andrés Juan, E. Pérez-Lebeña, *Int. J. Mol. Sci.* **2024**, *25*, 7314.
[5] A. Callejo, L. Sedó-Cabezón, I. Juan, J. Llorens, *Toxics* **2015**, *3*, 268–293.
[6] T. Peega, R. N. Magwaza, L. Harmse, I. A. Kotzé, *Dalton Trans.* **2021**, *50*, 11742–11762.
[7] J. M. J. Fréchet, D. A. Tomalia, *Dendrimers and Other Dendritic Polymers*, Wiley, Chichester, New York, **2001**, pp. 587–600, https://doi.org/10.1002/0470845821.
[8] R. J. Sarode, H. S. Mahajan, *J. Drug Deliv. Sci. Technol.* **2024**, *98*, 105896.
[9] E. F. Kangara, T. Peega, L. Harmse, D. C. Levendis, I. A. Kotzé, *New J. Chem.* **2019**, *43*, 3665–3672.
[10] I. B. Douglass, F. B. Dains, *J. Am. Chem. Soc.* **1934**, *56*, 719–721.
[11] G. T. Morgan, F. H. Burstall, *J. Chem. Soc.* **1934**, 965–971, https://doi.org/10.1039/jr9340000965.
[12] N. Taghavi Pourianazar, P. Mutlu, U. Gunduz, *J. Nanopart. Res.* **2014**, *16*, 2342.
[13] S. D. Santos, M. Xavier, D. M. Leite, D. A. Moreira, B. Custódio, M. Torrado, R. Castro, V. Leiro, J. Rodrigues, H. Tomás, A. P. Pêgo, *J. Controlled Release* **2018**, *291*, 65–79.
[14] M.-H. Li, S. H. Choi, T. P. Thomas, A. R. Desai, K. Lee, A. Kotlyar, M. M. Banaszak, J. R. Baker, *Eur. J. Med. Chem.* **2012**, *47*, 560–572.
[15] P. A. Barra, L. F. Barraza, V. A. Jiménez, J. A. Gavin, J. B. Alderete, *Struct. Chem.* **2014**, *25*, 1443–1455.
[16] A. M. Plutín, A. Alvarez, R. Mocelo, R. Ramos, O. C. Sánchez, E. E. Castellano, M. M. da Silva, W. Villarreal, L. Colina-Vegas, F. R. Pavan, A. A. Batista, *J. Braz. Chem. Soc.* **2018**, *29*, 1256–1267.
[17] I. A. Kotzé, W. J. Gerber, Y. S. Wu, K. R. Koch, *Dalton Trans.* **2013**, *42*, 3791–3801.
[18] A. M. Jolly, M. Bonizzoni, *Macromolecules* **2014**, *47*, 6281–6288.
[19] A. Buczkowski, S. Sekowski, A. Grala, D. Palecz, K. Milowska, P. Urbaniak, T. Gabryelak, H. Piekarski, B. Palecz, *Int. J. Pharm.* **2011**, *408*, 266–270.
[20] P. K. Maiti, T. Çağın, S.-T. Lin, W. A. Goddard, *Macromolecules* **2005**, *38*, 979–991.
[21] I. Posadas, L. Romero-Castillo, N. El Brahmi, D. Manzanares, S. Mignani, J.-P. Majoral, V. Ceña, *Proc. Natl. Acad. Sci. USA* **2017**, *114*, E7660–E7669.
[22] M. Fang, Y. Cheng, J. Zhang, Q. Wu, J. Hu, L. Zhao, T. Xu, *J. Phys. Chem. B* **2010**, *114*, 6048–6055.
[23] L. V. Amorim, M. I. R. Barbosa, H. Lira, L. de, H. C. Ferreira, *Mater. Res.* **2007**, *10*, 53–56.

[24] M. S. Bakshi, A. Kaura, *Colloids Surf. A* **2004**, *244*, 45–51.
[25] E. D. Vega, E. Vásquez, Jorge, M. A. Masuelli, *JPBPC* **2015**, *3* 12–18.
[26] M. Fang, J. Zhang, Q. Wu, T. Xu, Q. Zhang, *J. Phys. Chem. B* **2012**, *116*, 3075–3082.
[27] I. Matai, *Biomater. Sci.* **2015**, *3*, 457–468.
[28] A. Buczkowski, D. Waliszewski, P. Urbaniak, B. Palecz, *Int. J. Pharm.* **2016**, *505*, 1–13.
[29] J. Bruce, M.Sc. Thesis, Stellenbosch University, South Africa, **2005**.
[30] K. R. Koch, *Coord. Chem. Rev.* **2001**, *216–217*, 473–488.

Manuscript received: December 2, 2024